Spatial Immunometabolic Profiling of Non-Small Cell Lung Cancer Reveals Distinct Immune Exclusion Patterns and Functional Niches.

SITC 2025 Abstract # 11127 / Paper # 81

Alyssa Whitley[1+], Daniel Winkowski, PhD[2+], Yue Hou[1], Matthew Moore[1], Ritu Mihani, PhD[1], Regan Baird, PhD[2] and Katherine J. Hales, PhD[2],
(1) Akoya Biosciences, a Quanterix Company, Marlborough, MA, (2) Visiopharm Corp., Broomfield, CO.

AKOYA BIOSCIENCES® A Quanterix® Company

VISIOPHARM®

Background

The tumor microenvironment (TME) in non-small cell lung cancer (NSCLC) is shaped by both immune infiltration and metabolic reprogramming, which together modulate therapeutic response. We applied Akoya's PhenoCode™ Discovery IO60 Panel, combined with a spike-in PhenoCode Metabolic Module, to spatially characterize immunometabolic interactions in FFPE NSCLC samples, including both adenocarcinoma and squamous cell carcinoma (SqCLC) subtypes.

AI-powered image analysis and spatially resolved cellular phenotyping were performed using Visiopharm®, enabling high-dimensional, quantitative assessment of cell types and their spatial relationships within the immunometabolic contexture.

Methods

Experiments were performed on the PhenoCycler®-Fusion platform, which supports the simultaneous detection of 100+ markers per tissue section. This capability enabled us to spike in key metabolic markers—GLUT1, LDHA, HK1, G6PD, ASCT2, CPT1A, ATP5A, SDHA, and IDH2—without sacrificing panel resolution. These markers span major metabolic pathways, including glycolysis, oxidative phosphorylation, fatty acid oxidation, and glutamine metabolism.

Image analysis was conducted using Visiopharm's Phenoplex™ spatial tissue analysis software, enabling high-throughput single-cell segmentation, immune cell phenotyping, spatial proximity mapping, and co-expression analysis across millions of cells. This approach allowed us to resolve distinct immunometabolic niches in situ. Glycolytic tumor regions (GLUT1+, LDHA+) were associated with exclusion of CD8+ T cells and enrichment of FoxP3+ Tregs and CD163+ macrophages, while oxidative and FAO-rich zones (ATP5A+, CPT1A+) supported suppressive myeloid populations with reduced effector T cell presence. CD8+ T cells expressing metabolic fitness markers (HK1+, ATP5A+) and effector molecules (Granzyme B+, Perforin+) were confined to metabolically permissive regions.

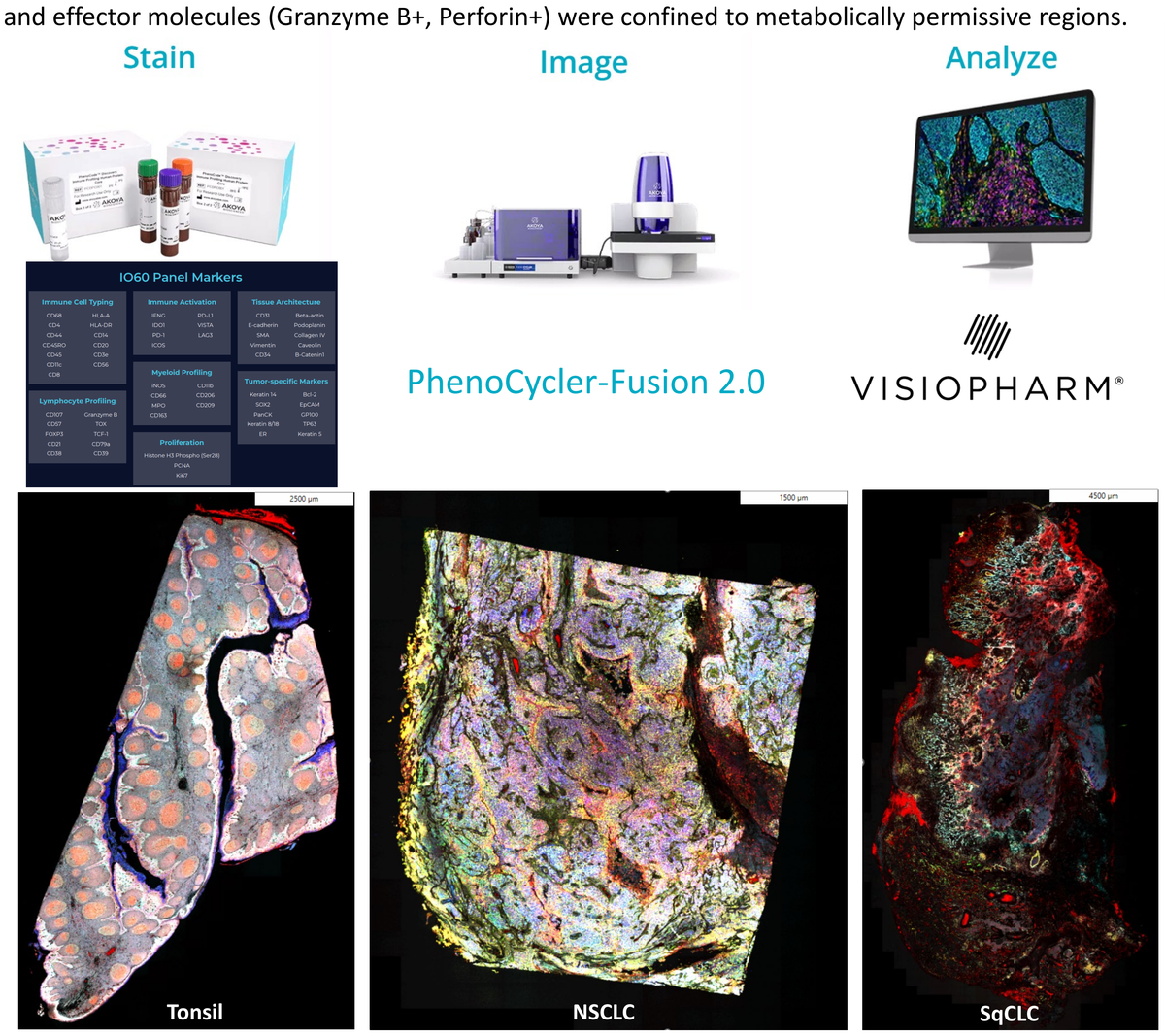

Figure 1. Overview of workflow from PhenoCode™ Discovery IO60 Panel staining, PhenoCycler-Fusion imaging and Visiopharm analysis platforms (top). Tissue images stained and displaying PhenoCode Metabolic Panel (bottom panel).

Visiopharm Image Analysis Workflow

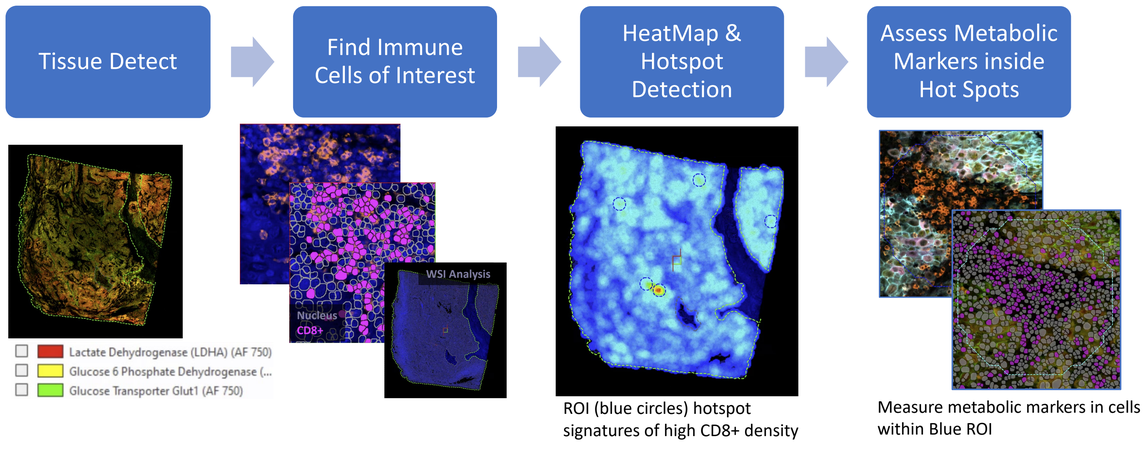

Figure 2. Overview of Image Analysis workflow from Visiopharm used to probe metabolic markers associated with high-density immune cell aggregates.

Results of Metabolic Marker Expression to Immune Cell Types

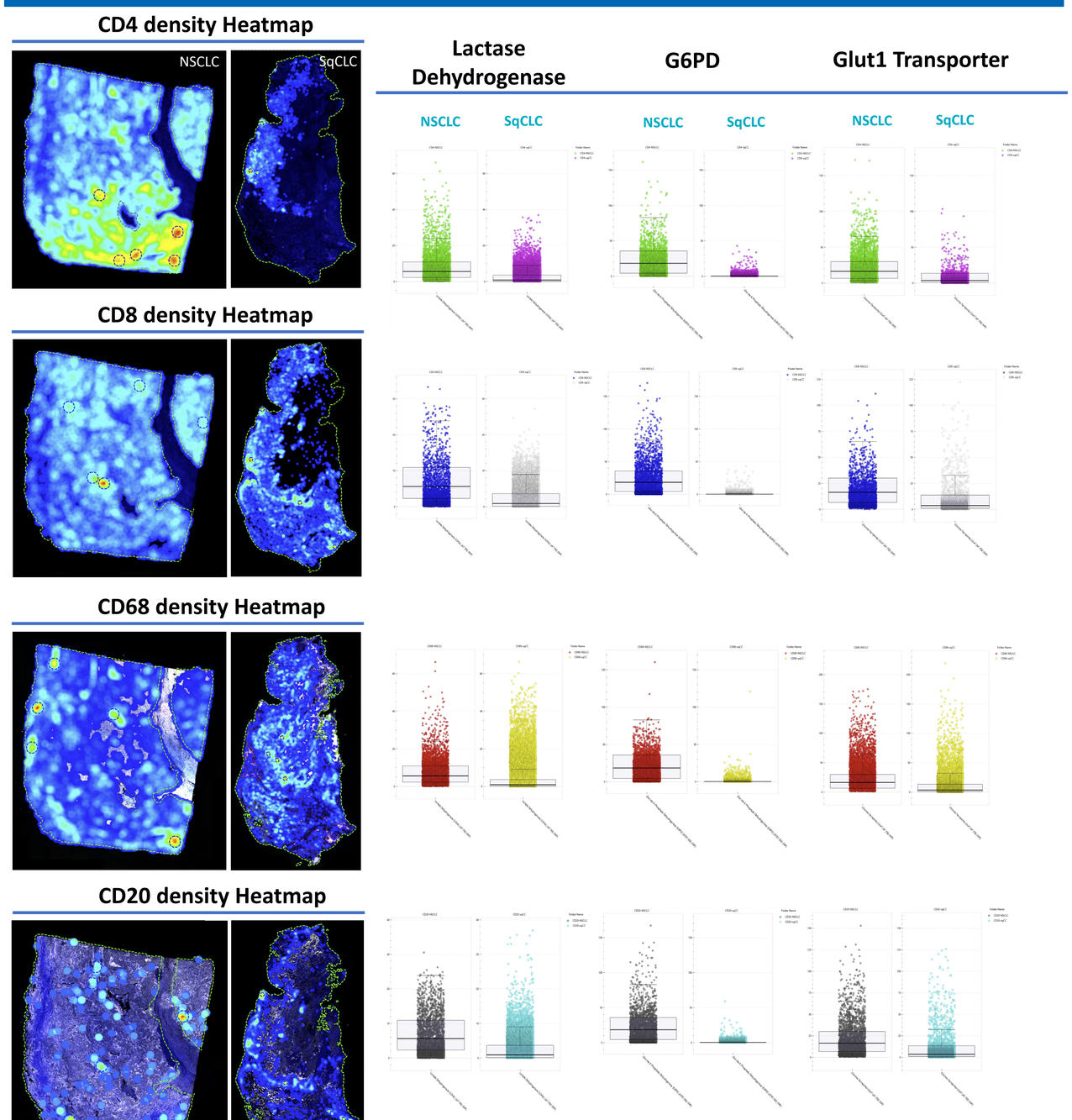

Figure 3. Selected immune cell density heatmap and their metabolic expression across NSCLC and SqCLC. Immune cell aggregate distribution varies across the tissue landscape with noted differences of G6PD in NSCLC over SqCLC.

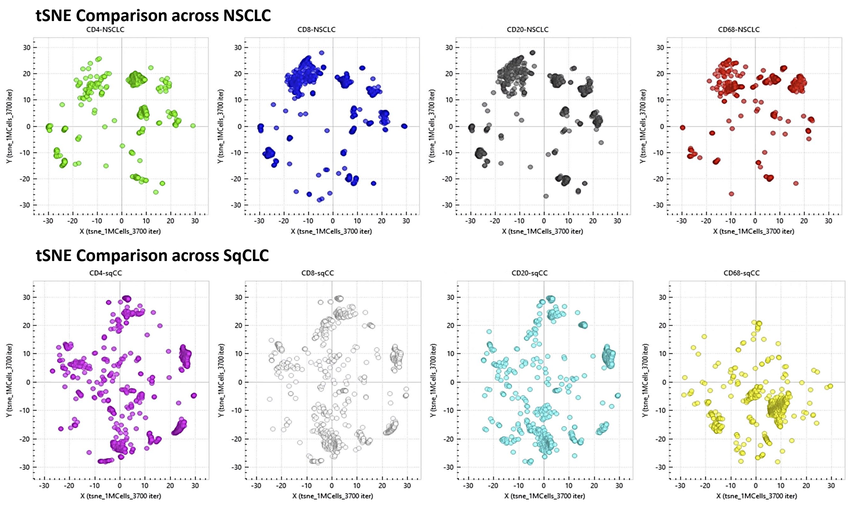

Figure 4. tSNE plots of immune cellular clusters within the ROIs across NSCLC and SqCLC tissues. Cellular cluster pattern differences exhibited in each tissue type indicates differences in cellularity is presente and are associated within the micro tissue domains.

Phenoplex Neighbor Counts

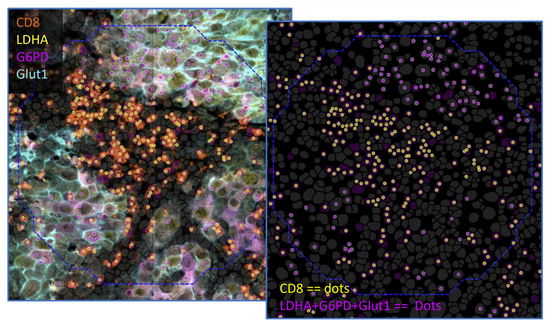

Co-occurrence matrix

	CD20 (AF 750) (MP)	CD4 (Cy5) (MP)	CD68 (Cy5) (MP)	CD8 (ATTO 550) (MP)	Dehydrogenase (G	nsporter Glut1 (A	rogenase (LDHA
Total	16970	57999	143745	48776	115794	302211	146194
CD20 (AF 750) (MP)	16970	1406	152	2514	10	232	391
CD4 (Cy5) (MP)	1406	57999	6110	3791	15379	23937	22702
CD68 (Cy5) (MP)	152	6110	143745	1938	12959	23075	29975
CD8 (ATTO 550) (MP)	2514	3791	1938	48776	4247	5801	4879
Glucose 6 Phosphate Dehydrogenase (G6PD) (ATTO 550) (MP)	10	15379	12959	4247	115794	69140	68241
Glucose Transporter Glut1 (AF 750) (MP)	232	23937	23075	5801	69140	302211	90420
Lactate Dehydrogenase (LDHA) (AF 750) (MP)	391	22702	29975	4879	68241	90420	146194

Neighborhood [0 – 30 um)

Target		G6PD+Glut1+LDHA+	Glut1+
CD8	NSCLC	3.00 +/- 5.35	7.20 +/- 6/79
	SqCLC	0.14 +/- 1.13	2.23 +/- 3.25
CD4	NSCLC	8.28 +/- 7.81	16.7 +/- 11.05
	SqCLC	0.04 +/- 0.24	1.31 +/- 2.21
CD68	NSCLC	4.86 +/- 5.60	22.29 +/- 12.90
	SqCLC	0.07 +/- 0.25	6.8 +/- 8.95
CD20	NSCLC	6.57 +/- 6.23	8.71 +/- 7.24
	SqCLC	0.06 +/- 0.26	2.37 +/- 5.68

Figure 5. Spatial neighbor counts of CD8+ cells with nearby G6PD+Glut1+LDHA+ cells or Glut+ only cells in glycolytic tumor regions, indicating potential differences in immune cell targets proximal to defined regions.

Conclusions

Comparative analysis revealed subtype-specific trends: adenocarcinomas displayed increased checkpoint expression (PD-1, PD-L1) in glycolytic zones, whereas SqCLC tumors exhibited broader FAO signatures and deeper immune exclusion. These findings underscore how spatial metabolic heterogeneity can shape immune cell function and distribution.

Together, this work demonstrates the power of combining ultrahigh-plex spatial proteomics with advanced spatial analysis via Visiopharm's AI-powered Phenoplex platform to uncover metabolic drivers of immune suppression. Spike-in strategies on the PhenoCycler-Fusion platform offer a flexible approach for integrated biomarker discovery in complex tissues.